

Evaluation of Transverse Construction Joints of Reinforced Concrete Beams

Dr.Qais Abdul-Majeed *

Received on: 17/11/2009

Accepted on: 6/5/2010

Abstract

Construction joints are stopping places in the process of placing concrete, and they are required because in many structures it is impractical to place concrete in one continuous operation. The amount of concrete that can be placed at one time is governed by batching and mixing capacity and by the strength of the formwork. A good construction joint should provide adequate flexural and shear continuity through the interface.

In this study, available experimental tests were analyzed by using a nonlinear three-dimensional finite element ANSYS computer program (v. 9). In addition an interface model was proposed for the transverse construction joints.

Six beams with different transverse construction joints at mid-span as well as to one reference beam without joint are analyzed. The reliability of the model is demonstrated by comparison with the experiment and alternative numerical analysis which shows 5-7% difference.

Keywords: construction joints, ANSYS, finite element method, reinforced concrete beams.

التقييم الإنشائي للمفاصل الإنشائية العمودية للعتبات الخرسانية المسلحة

الخلاصة:

إن المفاصل الإنشائية هي عبارة عن مناطق التوقف في عملية صب الخرسانة وهي ضرورية في عديد من المنشآت التي لا يمكن فيها صبا الخرسانة على مرحلة واحدة. إن مقدار الخرسانة التي يمكن صبها يعتمد على السعة الإنتاجية وسعة الخلط في الموقع وعلى مقاومة القالب. والمفصل الإنشائي الجيد يوفر استمرارية للقوى والانحناء (الانثناء) خلال السطح البيني. في هذه الدراسة تم تحليل نتائج عملية متوفرة باستخدام طريقة العناصر المحددة ثلاثية الأبعاد لاختبار لنقصي سلوك العتبات الخرسانية المسلحة والحاوية على المفاصل الإنشائية العمودية. بالاستفادة من برنامج ANSYS (صيغة 9). إضافة إلى اقتراح موديل لدراسة مناطق المفاصل العرضية. تم تحليل ستة من العتبات بوجود مفصل إنشائي عرضي في وسطها وواحدة بدون مفصل. ودقق مدى تطابق النموذج النظري بمقارنة النتائج العملية مع نتائج التحليل النظري، والتي أظهرت وجود اختلاف يتراوح بين 5 - 7%.

Introduction

Joints are necessary in concrete structures for a variety of reasons. Not all concrete in a given structure can be placed continuously, so there are construction joints that allow for work to be resumed after a period of time. Since concrete undergoes volume changes, principally related to shrinkage and temperature changes, it is desirable to provide joints and thus relieve tensile or compressive stresses that would be induced in the structure. It is necessary then to provide various types of joints in most concrete structures and in order that these joints adequately perform the functions for which they are intended it is essential for them to be installed and located correctly. In general, it is convenient to consider the various types of joints in two groups [1]:

- (a) **Functional Joints** which are installed to accommodate movement (volume changes) due to temperature, shrinkage during setting, expansion, sliding, warping, ...etc.
- (b) **Construction Joints** that are made when there is a break in the construction program.

Construction joints are stopping places in the process of placing concrete and they are provided to simplify construction of a structure, or even to make it possible and this depends on the type of work, the site conditions and the production capacity of the plant or labor employed. It frequently happens, when large volumes of concrete are being placed that there is a break in the construction work. Pure construction joints are not intended to accommodate movement

but they are merely separations between consecutive concreting operations and in fact, every effort is directed towards preventing movement from occurring at these joints.

Construction joints should not be confused with expansion joints that usually allow for free movement of parts of a structure and which are normally designed for complete separation. Construction joints are nearly always the weakest points in a structure. The main problem that remains is therefore in the formation of a good construction joint having the capability of providing a well bonded medium between the hardened and the fresh concrete. Thus construction joints in concrete structures should be placed where shear forces and moment (if possible) are expected to be low. Both the location and the size of joint should in general be chosen according to the type of structure to ensure good performance of the structure and to provide acceptable appearance.

In case of reinforced concrete beams, construction joints may be horizontal or vertical depending on the placing sequence prescribed by the design of the beam, Fig. (1). The main concern in joint placement is in providing adequate shear transfer and flexural continuity through the joint. Flexural continuity is achieved by continuing the reinforcement through the joint, while shear transfer is provided by shear friction between old and new concrete, or dowel action in reinforcement through the joint [2]. Construction joints may result in less than 100% of shear capacity and

should be made in the following manner [1,3]:

1. The surface of hardened concrete along the joint should be thoroughly roughened.
2. The surface of the concrete should then be cleaned thoroughly to remove all foreign and attached matter such as waste.
3. Hardened concrete should be moistened thoroughly before new concrete is placed on it.
4. No pool of water should be left standing on the wetted surface when new concrete is placed.

Bass et al. [4] studied the shear transfer across new and existing concrete interfaces by carrying out an experimental program, to provide information on the interface shear capacities between new concrete cast against an existing concrete surface. They concluded that an increase in the amount of reinforcement crossing the interface resulted in higher shear capacities at large slip levels. It was concluded that an increase in the embedment depth of the interface reinforcement resulted in an increase in the shear transfer capacity of the concrete interface.

Based on the **ACI 318M-08 Building Code** [5] the nominal shear friction strength V_n was given as:

$$V_n = \mu \times A_{vf} \times f_y \dots (1)$$

where:

V_n = nominal shear strength

μ = coefficient of friction along the interface

A_{vf} = area of shear-friction reinforcement

Clark and Gill [6] tested concrete prisms with cube strength with range

(24 to 66 MPa) to study the shear strength of smooth unreinforced construction joints. Results showed that shear was transmitted by combination of "cohesion" and "friction" and no dependence of strength upon age should be considered in design.

Ismail [7] cast ten reinforced concrete beams having rectangular cross section and tested as simply supported up to failure under the action of two point loads. Eight of these beams were designed to contain horizontal construction joints (HCJ) of different number and location in the beam while the other two beams had no construction joint. All the tested beams had been designed to fail in flexure and had same amount and type of longitudinal and transverse reinforcement as well as similar concrete properties. The results of this series of tests indicated that the presence of HCJ in reinforced concrete beams leads to a decrease in its cracking and ultimate loads and increase in its ultimate deflection while no appreciable change in the value of the beam deflection at first crack can be expected.

Mehrath [8] presented an experimental investigation to the flexural behavior of reinforced concrete (RC) beams containing a transverse construction joint (TCJ). Twenty three simply supported RC beams having a rectangular section (150mm x 250mm) and a span of (2m) were cast and tested under the action of two points loading. Three of these beams had no TCJ in them and were considered as reference beams while

each one of the other twenty beams had one TCJ in it. The variables considered in this experimental work were the location of the TCJ (either at mid-span or at the two-third point of the span of the beam), the shape of TCJ (vertical, 45° inclined, 60° inclined, joggle, or L shaped) and the presence of an additional stirrup inside TCJ. It was concluded that the best location for the TCJ should be at the mid-span which represents the location of minimum shear and maximum bending moment.

This study presents an attempt to use the finite element software ANSYS for analyzing simply supported reinforced concrete beams with construction joint. A comparison is made with available experimental results of Ref. [8]. The geometry and loading conditions for specimens is detailed in Fig. (2). For all the beams, the shear span - to - depth ratio was kept at 2.7. The joint was located at the midspan of the beam (in the middle third portion of the beam where there are zero shear and maximum bending moment). Four types of construction joint were considered in this study (vertical, inclined, joggle and L-shaped construction joint) as shown in Table(1).

The average concrete mean compressive strength was $f_{cu} = 32\text{MPa}$ for cubes, $f'_c = 26\text{MPa}$ for cylinders and the modulus of rupture $f_r = 3.8\text{MPa}$. The size and mechanical properties of the reinforcement are listed in Table(2).

Modeling Methodology and Finite Element Analysis Approach

FE analysis is performed using ANSYS [9], a general purpose finite

element program. The status transition of concrete from an un-cracked to cracked state and the nonlinear material properties of concrete in compression and steel as it yields cause the nonlinear behavior of the beams under loading. Newton-Raphson equilibrium iteration is used to solve nonlinear problem in ANSYS. In a linear analysis the size of the load increment does not affect the results at all. However, for a nonlinear analysis, in which FE structures start cracking and behave nonlinearly under a sufficiently large load, the load applied to the beams must be increased gradually to avoid non-convergence. Tolerances in both force and displacement criteria may have to be gradually increased during the loading history to attain convergence.

Material Modeling

Concrete:

The SOLID65 [9], three-dimensional (3D) reinforced concrete solid element, is used to represent concrete in the models Fig. (3). The element, using a $2 \times 2 \times 2$ set of Gaussian integration points, is defined by eight nodes having three translational degrees of freedom at each node as detailed in Fig. (4). This element is capable of cracking in tension and crushing in compression, although the crushing capability of the element is not used in this study. The most important implementation of the SOLID65 element is the proper definition of nonlinear material properties. The responses of concrete under loading are characterized by distinct nonlinear behavior. Complete stress-strain curves for concrete are

needed to accurately predict the whole range of beam behavior from service loading up to failure and post failure responses. Additionally, the descending branch is needed since a portion of the concrete compression zone is usually in this range of strains at the ultimate limit state. The stress-strain curve here is nearly linearly elastic up to the maximum tensile strength. After this point, the concrete cracks and the strength decreases gradually to zero [10]. The stress-strain behavior of concrete in compression and post-cracking adopted in this research is shown in Fig. (5).

Discrete and Embedded Representation of Reinforcement:

In the present research, the reinforcement is included within the properties of the 8-node brick elements (embedded representation) to include the reinforcement effect in the concrete structures as shown in Fig. (6). Reinforcing bars that are crossing the joint, were represented by using "link elements" (Discrete representation). The LINK8, 3-D spar element, is used to represent the reinforcing steel bar. It is a uniaxial tension-compression element that can also include nonlinear material properties with two nodes having three degrees of freedom at each node. The stress-strain behavior can be assumed to be identical in tension and compression [11]. In the current study, a bilinear isotropic uniaxial stress-strain relationship is used for steel reinforcement as shown in Fig. (7).

Interface Finite Element Idealization:

Under static loading, a construction joint is modeled by a medium of negligible thickness called an "Interface", which represents two surfaces that are in a state of physical contact but may slide relative to each other. Construction joints in beams, columns, and walls can present a potential weakness if large shear forces need to be transmitted across them [12]. The shear capacity of the interface could be influenced by the type of surface penetration used for the joint. Shear may be transferred by means of friction when there is normal compressive stress acting on the interface. This normal stress may be due either to an externally imposed load or to reinforcing bars crossing the interface [13]. The interaction, or stress transfer between two concretes cast at different time obviously occurs via the following components [14]:

- I. Chemical adhesion.
- II. Friction caused by direct bearing of small asperities projecting from the faces of the joint.
- III. Dowel action of the reinforcement crossing the joint.

Two combined interface models are tried in this study. The first interface is capable of supporting only compression forces in the direction normal to the interface surface and shear (Coulomb friction) in the tangential direction. The second uses the normal and tangential (or dowel) stiffness of the transversely crossing bars.

Shear-Friction Modeling:

The behavior at junction or interface between structural materials involves relative translational motions under static loading [15]. In the context of numerical methods such as the finite element method, an interface or joint elements are used in order to account for the relative motions and associated deformation modes.

A three-dimensional point-to-point contact element [9] is used to model the nonlinear behavior of the surface between two concretes cast at different times. This model also includes the definition of the stress transfer. The element joins two surfaces that may maintain or break physical contact and may slide relative to each other. Also, the element is capable of supporting only compression in the direction normal to the interface between the two surfaces and Coulomb shear-friction in the tangential direction.

The 3-D point-to-point contact element has three degrees of freedom at each node (u , v and w) in the element coordinate system. The orientation of the interface is defined by the node locations. The interface is assumed to be perpendicular to $I-J$ line, as shown in Fig. (8).

In the basic Coulomb friction model, the two contacting surfaces can carry shearing stress up to a certain magnitude across their interface before they start sliding relative to each other. This state is known as sticking. Once the shearing stress is exceeded, the two surfaces will slide relative to each other. This state is known as sliding. The sticking – sliding calculations determine when a point is transferred

from sticking to sliding or vice versa as shown in Fig. (9) [9].

Dowel Action Modeling:

It is necessary to include the shear transfer mechanism of the dowel bars that are crossing the joint. The dowel action (shearing and flexure of the bars) will contribute to the overall shear stiffness at the joint interface.

To include this mechanism, the nonlinear spring element [9] is used. This element is a unidirectional element with nonlinear generalized force-deflection capability. The element has longitudinal capability with up to three degrees of freedom at each node (translations in the nodal x , y and z directions). The element is defined by two nodes. The geometry, node locations, and the nonlinear force-deflection for this element are shown in Fig. (10).

Finite element model

The finite element models that have been adopted in this study have a number of parameters, which can be classified in two categories:

- I. Material properties parameters, Table (3) [5, 10].
- II. Nonlinear solution parameters, Table (4) [10].

Finite element mesh for the tested beams are shown in Figs (11) to (16).

Experimental and theoretical results comparison

Both experimental and theoretical load-deflection curves show an initial apparent linear trend, after which the reduction of the beam stiffness indicates that yielding occurs. Load-deflection curves are shown in Figs.(17) to (23) for all analyzed

beams. The comparison between the load-deflection curves shows a basic agreement up to the yielding load, which indicates that the model used was efficient. It is noted that the experimental ultimate deflection was greater than the estimated theoretical values. This, as expected, may be due to inaccuracies in measuring deflection during testing, mainly due to continuous increase in deflection values when reaching the ultimate load.

Table (5) gives the experimental and theoretical failure loads which indicate that the difference is only between 5.77-6.83% .

The Joggle shape connection gave better behavior prediction than the others. This better load-deflection performance of beam B7 can be attributed to the better behavior of the Joggle shape connection –better interlocking between the old and new concrete, Fig. (24). This figure shows that the smallest load capacity was due to the joint failure in the case of 45° inclined shape connection.

Theoretical results of adding additional one stirrup at the joint for the beams with Joggle connection were indicated in Fig. (25), which indicated increased load capacity by 2.4%.

Conclusions

The results obtained for the beams that are chosen to verify the accuracy and the validity of the adopted models show that the nonlinear finite element method of analysis is a powerful and relatively economic tool for predicting the structural response and the load carrying capacity of reinforced concrete members. The use of interface

elements in connecting the concrete brick elements at the location of the construction joint is necessary to simulate the weakness of the joint and to assess the way the stresses will transfer through the joint. The beams with Joggle joint type gave higher load carrying capacity by 2.4% than the others. Adding one additional stirrup across the vertical joint improves the performance of the jointed beam, as well as strength the joint and arrests any possible crack propagation.

The shape of the transverse construction joint affected the structural behavior of jointed reinforced concrete beams-with respect to strength, ductility and mode of failure.

References

- [1] Critchell P., “*Joints and Cracks in Concrete*”, CR Books (A MacLaren Company), London, 1968.
- [2] ACI Committee Report 224.3R-95 “*Joints in Concrete Construction*”, pp.1- 44, 1995.
- [3] Fintel M., “*Joints in Buildings*”, Handbook of Concrete Engineering, 2nd Edition, pp.121, 1985.
- [4] Bass R., Carrasquillo R., and Jirsa J., “*Shear Transfer Across New and Existing Concrete Interfaces*”, ACI Structural Journal, vol.86, no.4, July – Aug. 1989.
- [5] ACI Committee 318, “*Building Code Requirements for Structural Concrete (ACI 318M-08) and Commentary (ACI 318RM-08)*”, American Concrete Institute, Farmington Hills, U.S.A., 2008.
- [6] Clark L. and Gill B., “*Shear Strength of Smooth Unreinforced*

- Construction Joints" Magazine of Concrete Research, vol. 37, no. 131, pp. 95-100, June 1985.
- [7] Ismail A.K., "Flexural Behavior of Reinforced Concrete Beams having Horizontal Construction Joints", M.Sc. Thesis, University of Technology, April 2005.
- [8] Mehrath H. J. "Flexural Behavior of Reinforced Concrete Beams having Transverse Construction Joints", M.Sc. Thesis, University of Technology, Feb. 2008.
- [9] "ANSYS Manual", Version 9.0, U.S.A., 2006.
- [10] Chen W., "Plasticity In Reinforced Concrete", McGraw-Hill Book Company, U.S.A., pp.592, 1982.
- [11] Al- Manasser A., and Phillips D., "Numerical Study of Some Post Cracking Material Parameters Affecting Nonlinear Solutions in Reinforced Concrete Deep Beams", Canadian Journal of Civil Engineering, vol.14, pp.655–666, April 1987.
- [12] Park R. and Paulay T., "*Reinforced Concrete Structures*", John Wiley & Sons, pp.319 – 332, U.S.A., 1975.
- [13] Tassios H. and Vintzeleou E, "*Concrete -to- Concrete Friction*", Journal of Structural Engineering, ASCE, vol.113, no.4, pp.832- 849, April 1987.
- [14] Mattock A., "*Cyclic Shear Transfer and Type of Interface*", Journal of the Structural Division, ASCE, vol.107, no. ST10, pp. 1945-1964, October 1981.
- [15] Desai C. and Zaman M., "Thin-Layer Element for Interfaces and Joints", International Journal for Numerical and Analytical Methods in Geomechanics, vol.8, pp.19 – 43, 1984.

Table (1) Summary of the tested beams

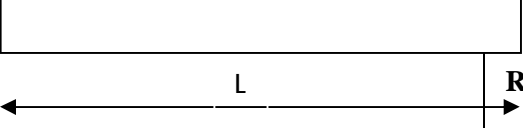
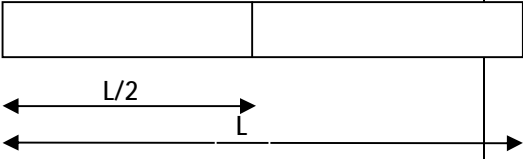
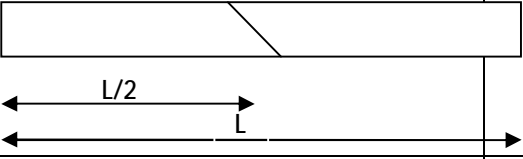
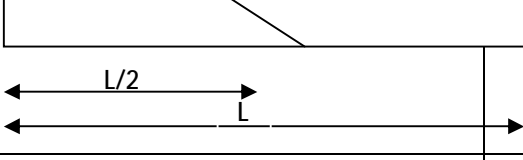
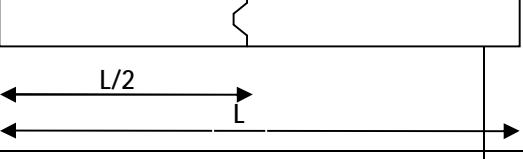
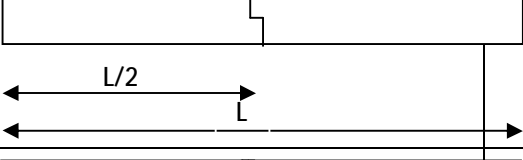
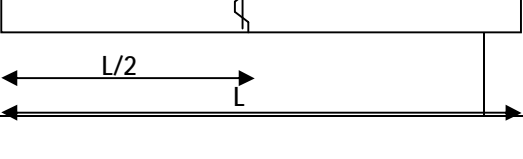
Beam mark	Shape and location of T.C.J	Description
B1		Reference beam(No TCJ)
B4		No additional stirrup inside the TCJ
B5		Ditto
B6		Ditto
B7		Ditto
B8		Ditto
B12		one-Ø5mm additional stirrup inside the TC

Table (2) Properties of the steel reinforcement used in the tested beams

Type of reinforcement in the tested beams	Diameter (mm)	f_y (MPa)	f_u (MPa)	E (MPa)
Shear reinforcement	5	380	425	200000
Longitudinal bars (in compression)	8	420	519	200000
Longitudinal bars (in tension)	12	425	530	200000

Table (3) Material property parameters

	Name	Definition	Value
Concrete	E_c	Young's modulus (MPa)	$4700\sqrt{f'_c}$
	f_t	Tensile strength (MPa)	$0.33\sqrt{f'_c}$
	ν	Poisson's ratio	0.2 [*]
Interface	μ	Coefficient of friction	1 [*]
Steel	E_s	Young's modulus (MPa)	200000 [*]
	ν	Poisson's ratio	0.3 [*]

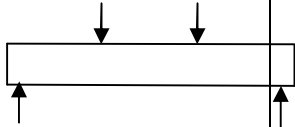
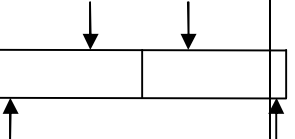
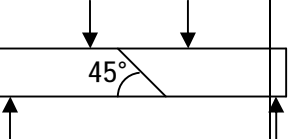
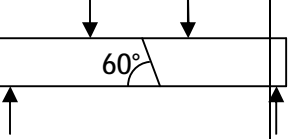
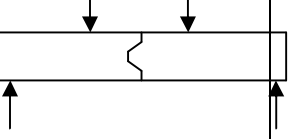
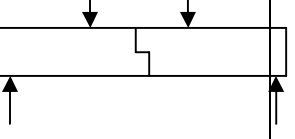
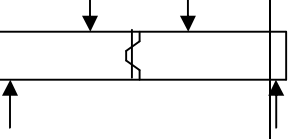
- Assumed value

Table (4) Nonlinear solution parameters

Name	Definition	Value
f_{cb}	Ultimate biaxial compressive strength	$1.2 f'_c$
σ_h^a	Hydrostatic stress	$1.157 f'_c$
f_1	Ultimate compressive strength for a state of biaxial compression superimposed on (σ_h^a)	$1.45 f'_c$
f_2	Ultimate compressive strength for a state of un-axial compression superimposed on (σ_h^a)	$1.725 f'_c$
α_1	Tension stiffening parameters	60^*
α_2		0.6^*
β_o	Shear transfer parameters	$0.0 - 1.0$
β_c		$0.0 - 1.0$
E_w	Steel hardening parameter	$0.02 E_s^*$

* Assumed values

Table (5) Test results for the tested beams

Beam Mark	Shape of the beam	Pu (exp.) kN	Pu (theo.) kN	Percent difference%	Mode of Failure
B1		81.5	76.8	5.77	Flexural Failure
B4		80	74.88	6.4	Flexural Failure
B5		70	65.28	6.74	Joint Failure
B6		79	74	6.33	Flexural Failure
B7		80.5	75	6.83	Flexural Failure
B8		80	74.97	6.3	Flexural Failure
B12		81.5	76.6	6.01	Flexural Failure

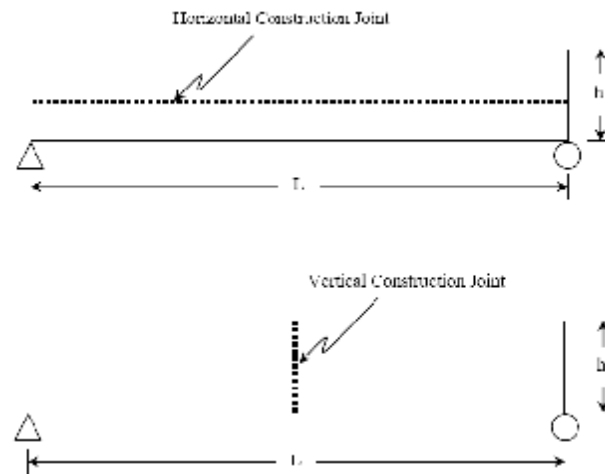


Figure (1) Construction joints type.

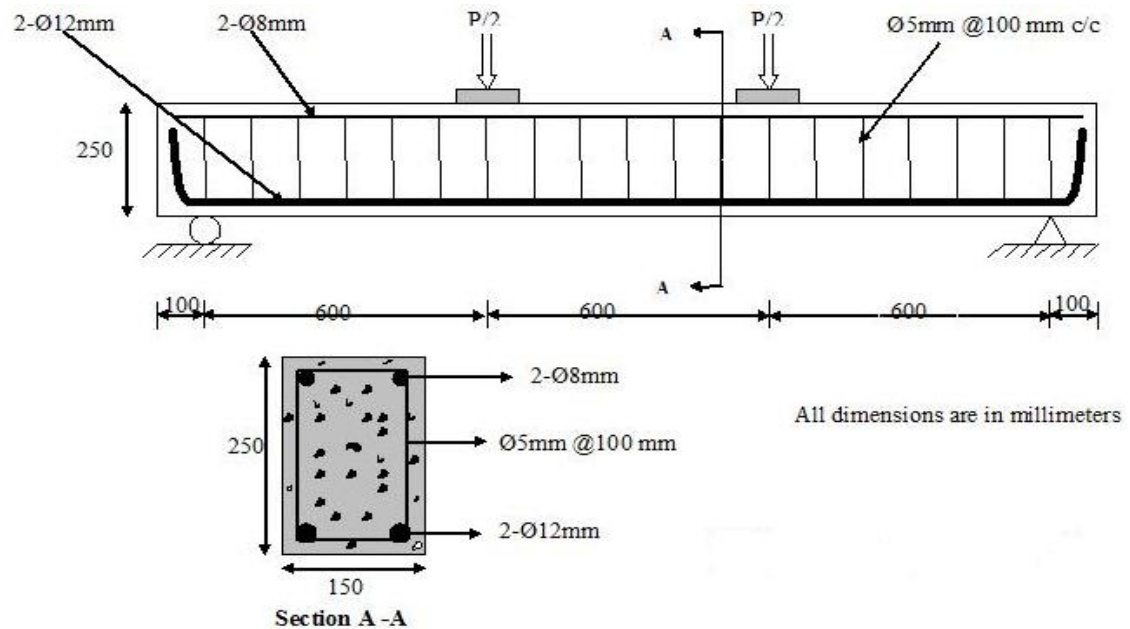
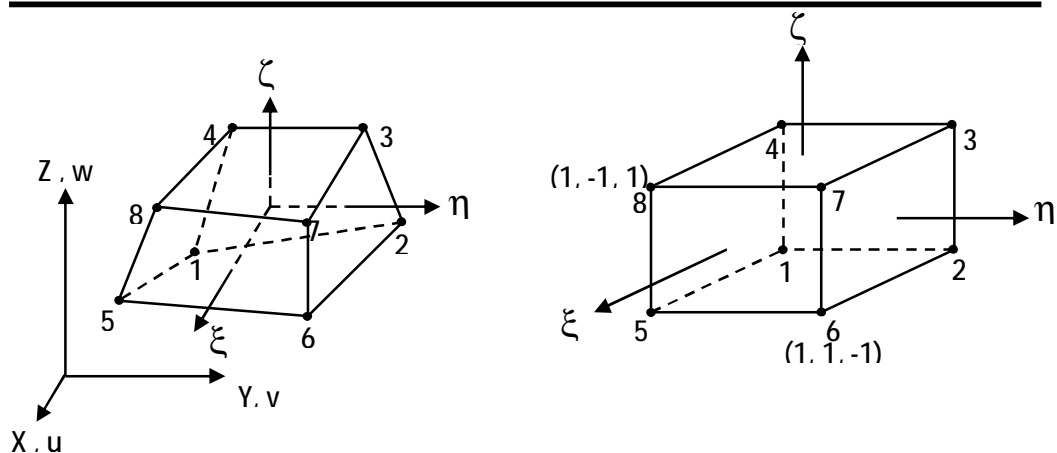


Figure (2) details of the tested beams[8].



b) 8-node Brick Element in Local

Figure (3) Three-dimensional 8-node brick element [9].

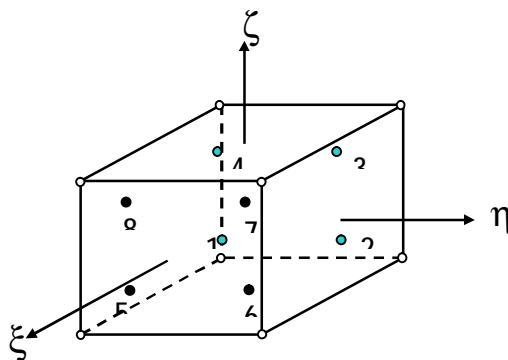


Figure (4) Distribution of integration points [9].

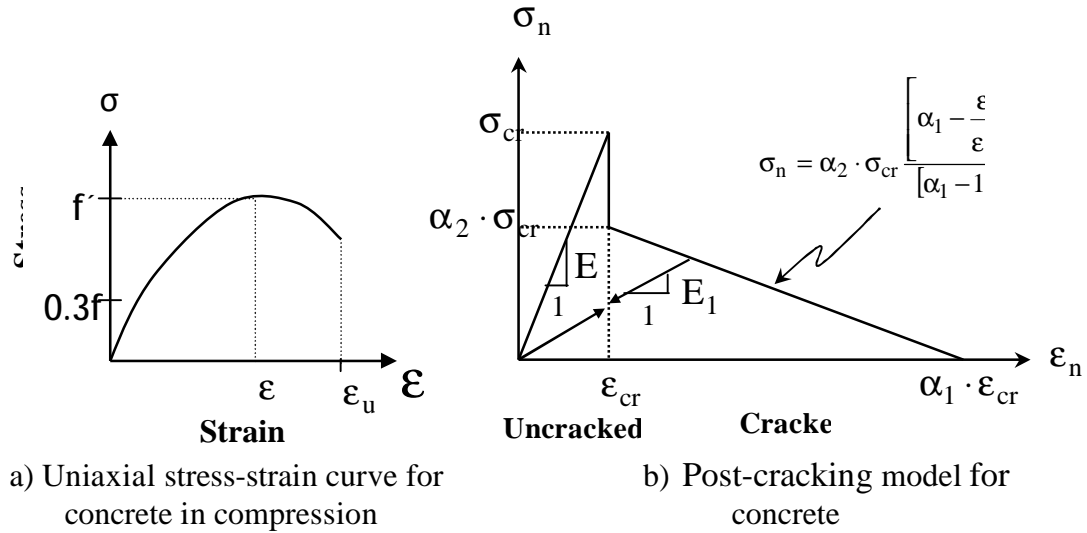


Figure (5) Concrete stress-strain curve [10].

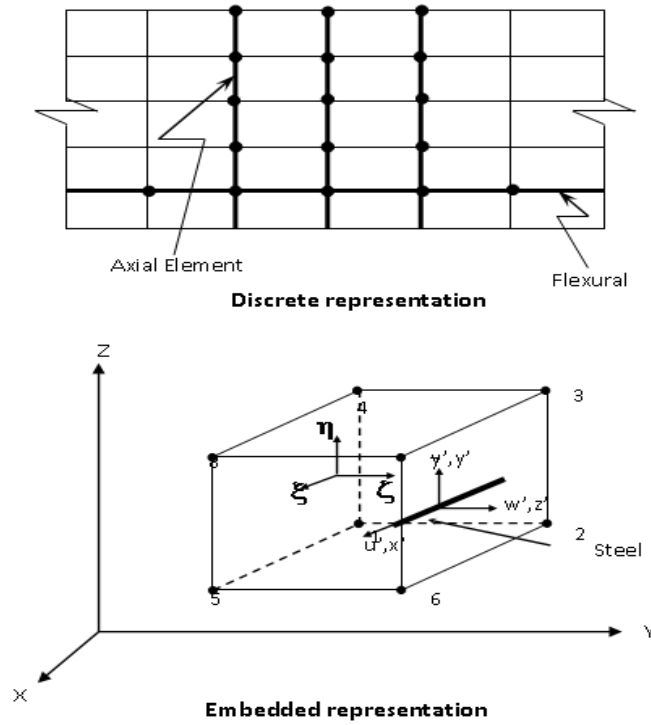


Figure (6) Reinforcement representation types [9].

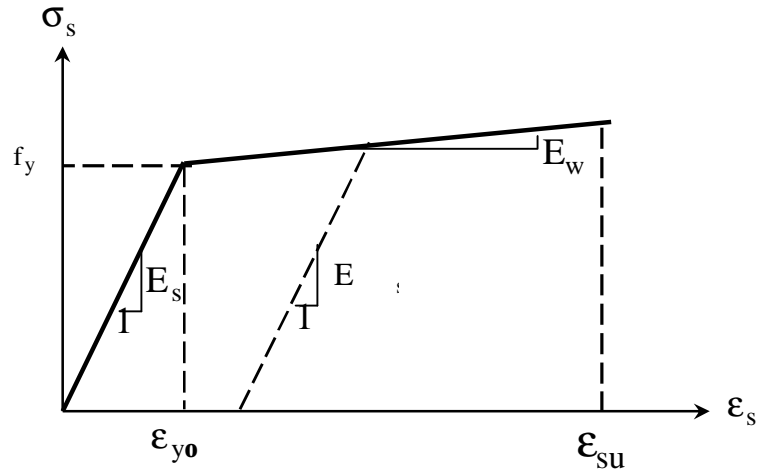


Figure (7) Stress – strain relation-ship of steel bar [12].

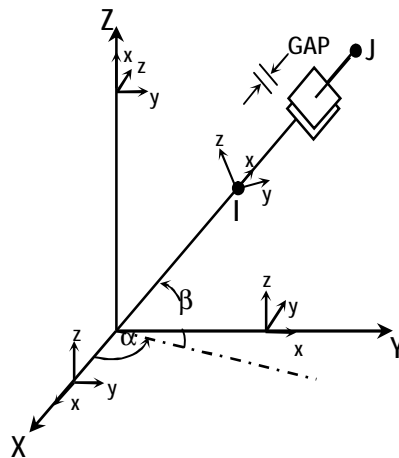


Figure (8) 3-D Point-to-point contact Element[9].

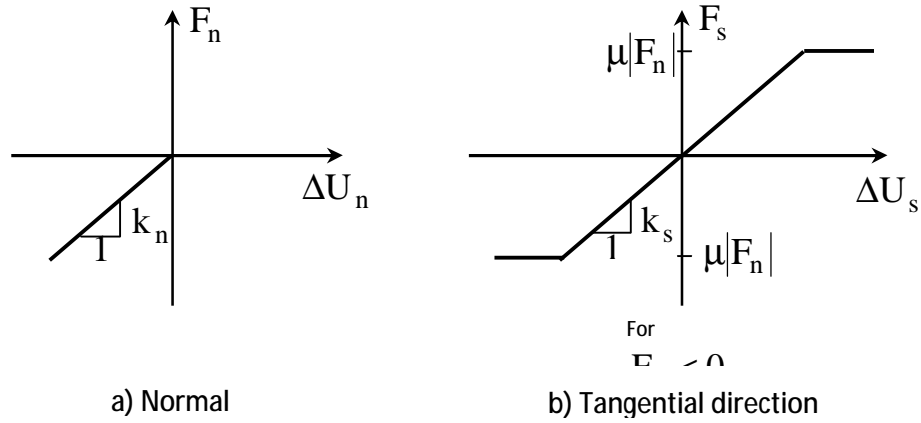


Figure (9) Nonlinear spring element[9].

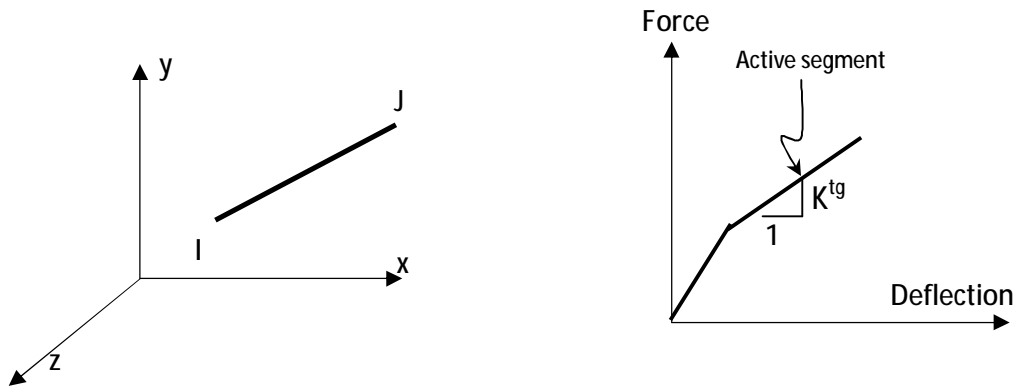


Figure (10) Interface force– deflection relation-ship [9]

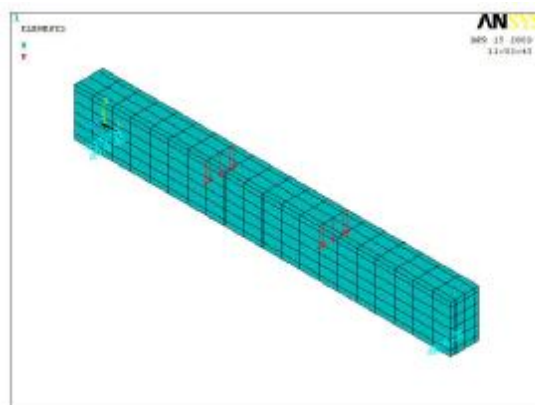
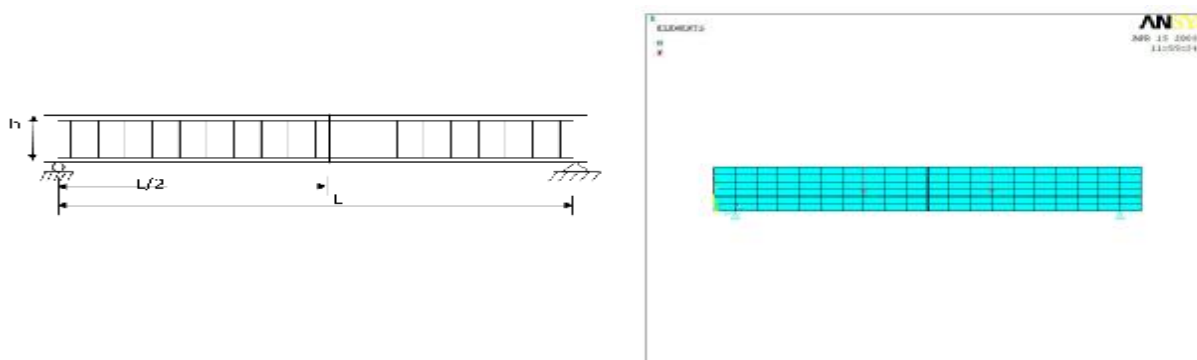


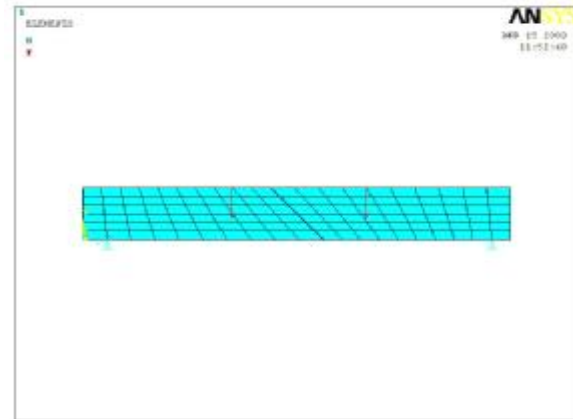
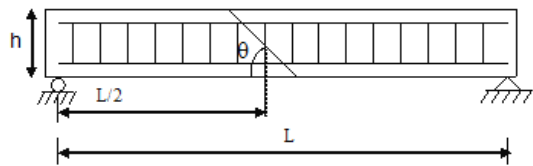
Figure (11) Finite element mesh for the tested beam B1.



a) details of tested beam B4

b) mesh of beam B4

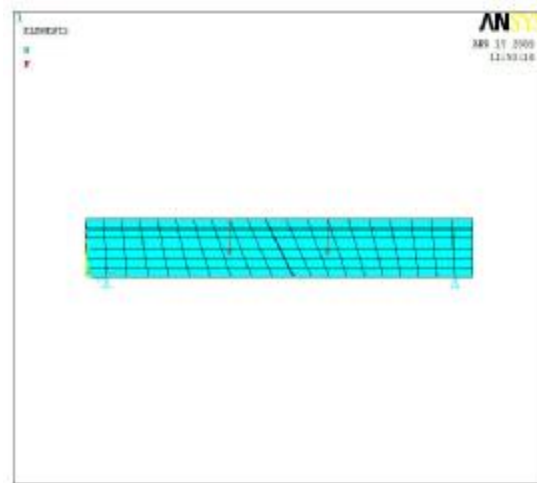
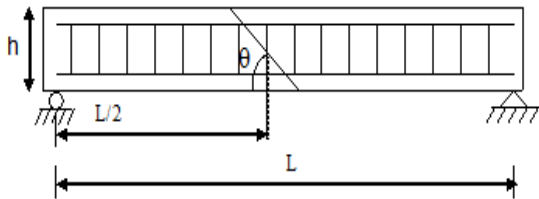
Figure (12) Finite element mesh for tested beam B4 .



a) details of tested beam B5

b) mesh of beam B5

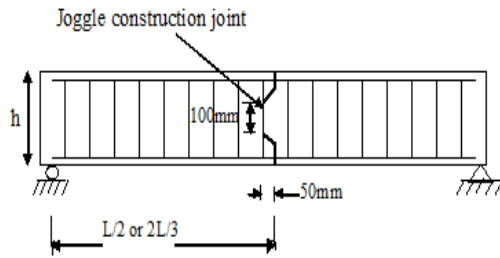
Figure (13) Finite element mesh for tested beam B5



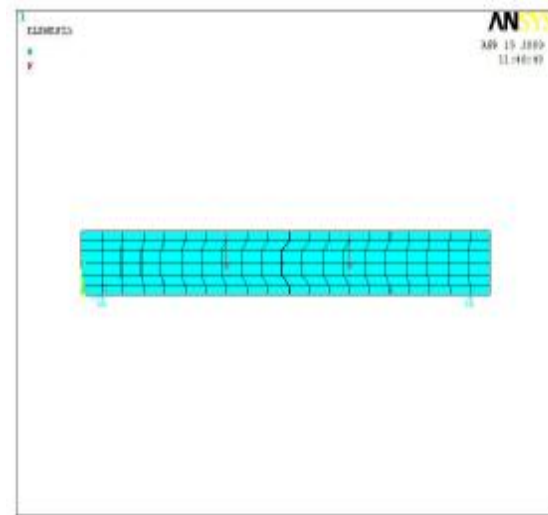
a) details of tested beam B6

b) mesh of beam B6

Figure (14) Finite element mesh for the tested beam B6.

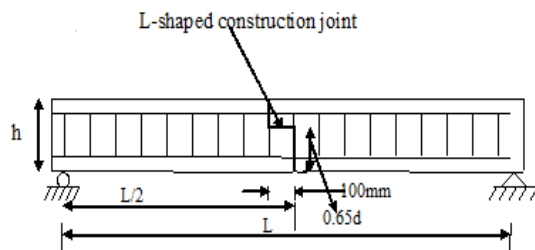


a) details of tested beam B7

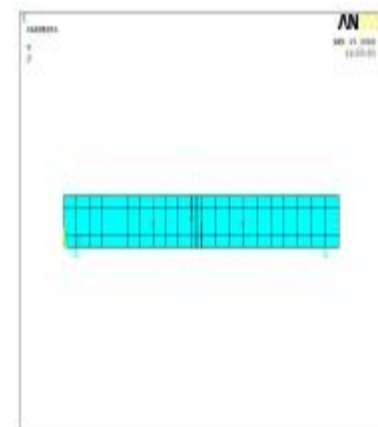


b) mesh of beam B7

Figure (15) Finite element mesh for the tested beam B7.



a) details of tested beam B8



b) mesh of beam

B8

Figure (16) Finite element mesh for the tested beam B8.

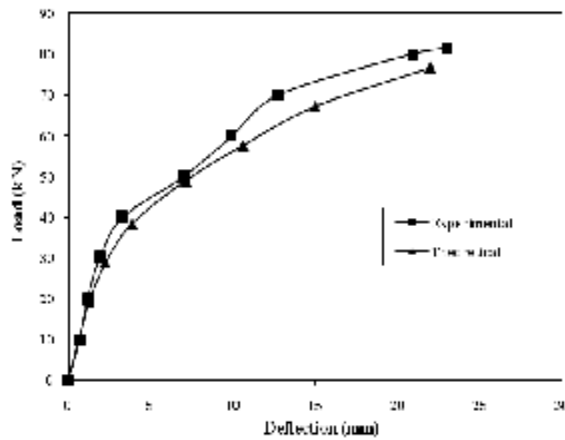


Figure.(17): Load-deflection curves for beam B1

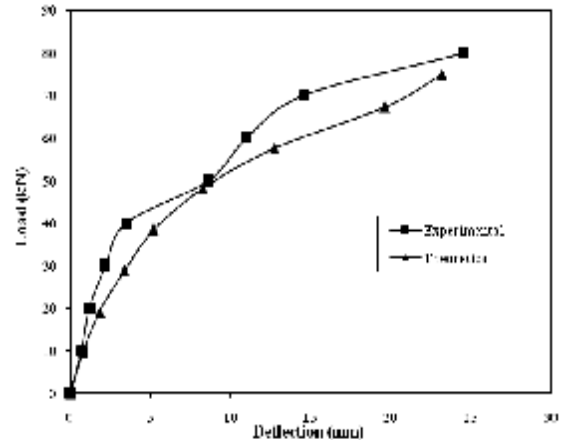
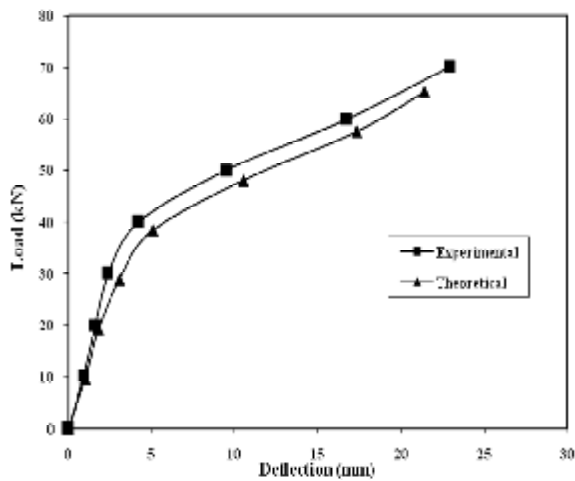
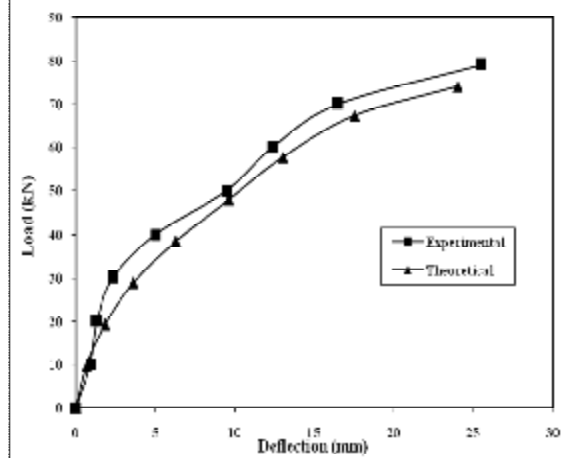


Figure.(18): Load-deflection curves for beam B4.



Figure(19): Load-deflection curves for beam B5



Figure(20): Load-deflection curves for beam B6

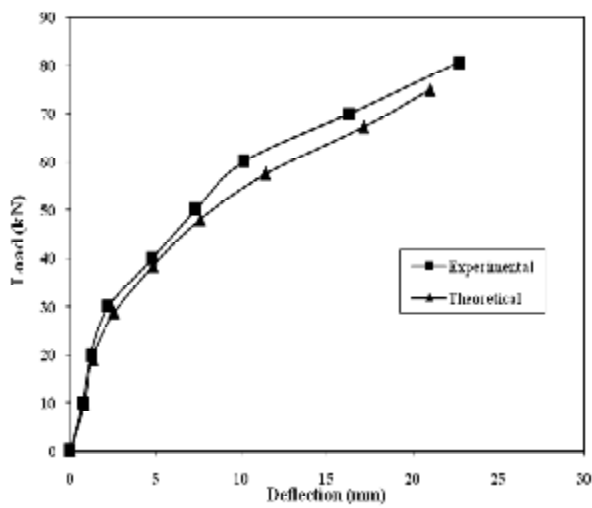


Figure (21) Load-deflection curves for beam B7

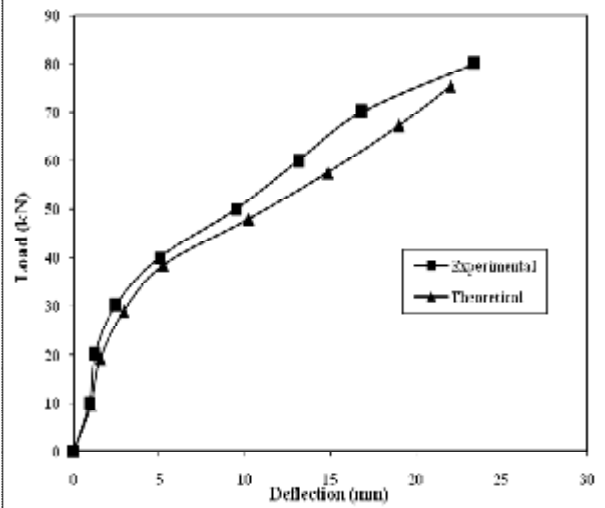


Figure (22) Load-deflection curves for beam B8

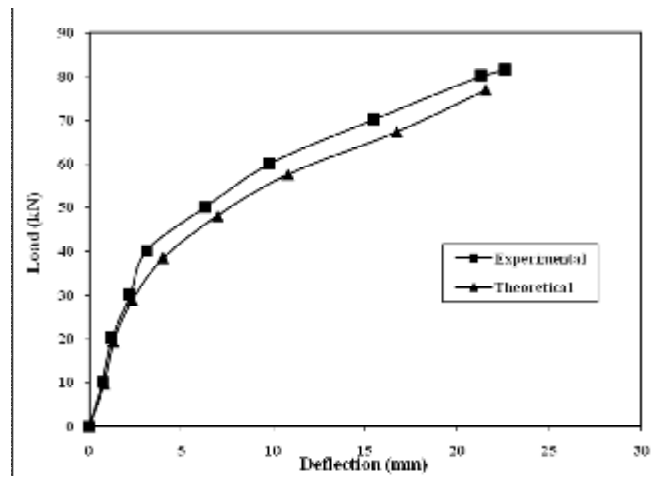


Figure (23) Load-deflection curves for beam B12

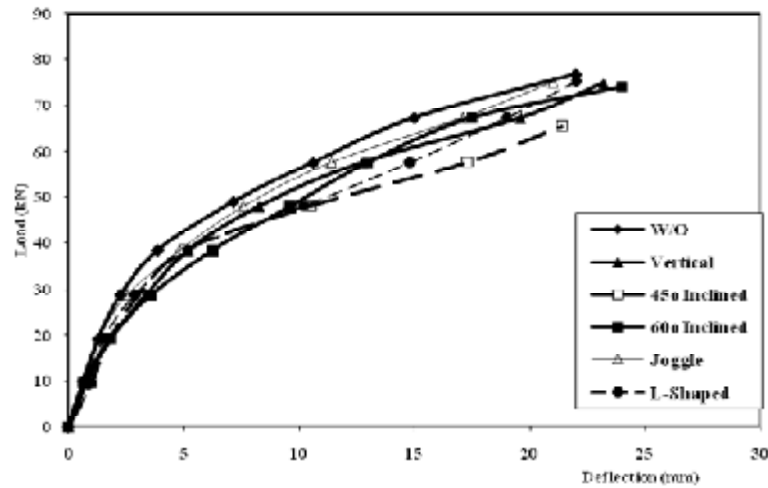


Figure (24) Theoretical load-deflection curves for all beams

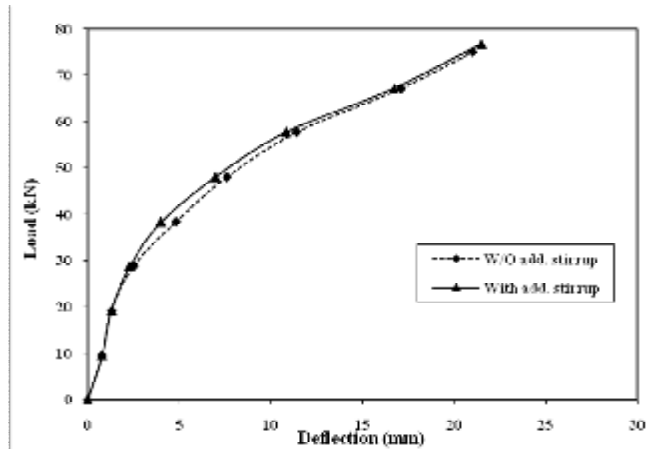


Figure (25) Theoretical load-deflection curves for beam B12